Published in final edited form as:
Biochem Biophys Res Commun. 2012 March 9; 419(2): 333–338. doi:10.1016/j.bbrc.2012.02.024.

POST-TRANSLATIONAL MODIFICATION OF OSTEOPONTIN: EFFECTS on *in vitro* HYDROXYAPATITE FORMATION and GROWTH

Adele L. Boskey[a], **Brian Christensen**[b], **Hayat Taleb**[a], and **Esben S. Sørensen**[b]

Adele L. Boskey: Boskeya@hss.edu; Brian Christensen: bc@mb.au.dk; Hayat Taleb: Talebh@hss.edu; Esben S. Sørensen: ess@mb.au.dk

[a]Musculoskeletal Integrity Program, Hospital for Special Surgery, New York, NY

[b]Department of Molecular Biology and Genetics, Aarhus University, Denmark

Abstract

The manuscript tests the hypothesis that posttranslational modification of the SIBLING family of proteins in general and osteopontin in particular modify the abilities of these proteins to regulate in vitro hydroxyapatite (HA) formation. Osteopontin has diverse effects on hydroxyapatite (HA) mineral crystallite formation and growth depending on the extent of phosphorylation. We hypothesized that different regions of full-length OPN would also have distinct effects on the mineralization process. Thrombin fragmentation of milk OPN (mOPN) was used to test this hypothesis. Three fragments were tested in a *de novo* HA formation assay; an N-terminal fragment (aa 1–147), a central fragment (aa 148–204) denoted SKK-fragment and a C-terminal fragment (aa 205–262). Compared to intact mOPN the C- and N-terminal fragments behaved comparably, promoting HA formation and growth, but the central SKK-fragment acted as a mineralization inhibitor. In a seeded growth experiment all fragments inhibited mineral proliferation, but the SKK-fragment was the most effective inhibitor. These effects, seen in HA-formation and seeded growth assays in a gelatin gel system and in a pH-stat experiment were lost when the protein or fragments were dephosphorylated. Effects of the fully phosphorylated protein and fragments were also altered in the presence of fibrillar collagen. The diverse effects can be explained in terms of the intrinsically disordered nature of OPN and its fragments which enable them to interact with their multiple partners.

Keywords

Osteopontin; hydroxyapatite; SIBLING proteins; mineralization mechanisms

Corresponding Author: Adele L. Boskey, Hospital for Special Surgery, 535 E 70th Street, New York, NY 10021, USA, Phone: 212 606 1453, Boskeya@HSS.edu.

None of the authors have any conflict of interest to declare.

INTRODUCTION

Osteopontin (OPN) is a member of the "SIBLING" (small integrin binding ligand N-glycosylated) family proteins found in relatively high concentrations in odontoblasts, osteoblasts and osteocytes [1,2]. It is well accepted that OPN is important for regulation of biomineralization. For example, phosphorylated bone OPN in cell-free *in vitro* systems [3–6] and in cell culture [7–10] inhibits hydroxyapatite (HA) mineral deposition. In contrast, the highly phosphorylated milk OPN (mOPN) promotes mineralization in solution [11]. A small synthetic OPN peptide (aa 115–132) containing the acidic, serine- and aspartate-rich motif (ASARM) also inhibits HA formation and growth in a phosphorylation dependent manner [12]. In the OPN-deficient (OPN-KO) mouse mineralization is enhanced in bones, calcified cartilage [13], vasculature [14], and kidneys [15]. Recently an antibody to a small peptide adjacent to the thrombin cleavage site near the integrin binding RGD sequence of OPN was shown to block kidney calcification in mice [16] implying that this OPN domain is important in the mineralization process. It is our underlying hypothesis that post-translational modifications including phosphorylation and fragmentation of the SIBLING proteins in general, and of OPN in particular, determines their ability to regulate HA formation. It has previously been shown that full length (fl)-DMP1 is an inhibitor of HA formation and growth [17], while its N- and C- terminal fragments are mineralization promoters and a N-terminal proteoglycan form an inhibitor. In contrast, fl-MEPE is a promoter of HA formation and the fragments are inhibitors [18]. Although the intact product of the *dspp* gene has not be isolated, its two fragments, phosphophoryn and dentin sialoprotein, both SIBLING proteins, both act as HA promoters but the effect of phosphophoryn is much greater than that of dentin sialoprotein [19,20]. To extend this information to another SIBLING the purpose of this study was to compare the effects of fragments of OPN on HA formation and growth. Since the phosphorylation and enzymatic cleavage of mOPN is well characterized [21–23] this study was performed with fl-mOPN and three thrombin generated mOPN fragments (Figure 1).

MATERIALS & METHODS

Purification and Thrombin-Cleavage of mOPN

OPN was purified from bovine milk as previously described [24]. For generation of N-terminal, central and C-terminal fragments, purified mOPN was incubated with bovine thrombin (10 mU thrombin/ug mOPN) (GE Healthcare, Uppsala, Sweden) in 0.1 M ammonium bicarbonate at 37°C for 1 hr; resulting fragments separated on a Superdex Peptide HR 10/30 column (GE Healthcare) yielding two peaks, one containing the N-terminal part (aa 1–147), the other containing the central part (aa 148–204) and the C-terminal part (aa 205–262). The central and C-terminal fragments were separated by reverse-phase HPLC on a Vydac C_{18} column (Separations Group, Hesperia, CA) connected to a GE Healthcare LKB system. Separation was carried out in 0.1% trifluoroacetic acid and fragments were eluted with a linear gradient of 75% propan-2-ol in 0.1% trifluoroacetic acid. All peaks from the different purification steps were analyzed by mass spectrometry (MS) and N-terminal sequencing. Purified fragments were quantified with a micro BCA protein assay kit (Pierce, Rockford, IL) and lyophilized.

Dephosphorylation of mOPN

OPN fragments were incubated with bovine alkaline phosphatase (ALP) (Sigma) (20mU ALP/μg protein) in 10 mM ammonium bicarbonate (pH 8.5) overnight at 37 °C and subsequently analyzed by MS (Voyager DE-PRO MALDI-TOF mass spectrometer (Applied Biosystems)). All spectra were obtained in positive linear-ion mode using a nitrogen laser at 337 nm and an acceleration voltage of 20 kV. Typically, 50–100 laser shots were added per

spectrum and calibrated with external standards. The molecular sizes of each of the phosphorylated and dephosphorylated fragments (Table 1) were used to calculate the molar content for each experiment.

Effect of mOPN Fragments on HA Formation and Growth

HA crystals were prepared from amorphous calcium phosphate at pH 7.4 for 24 hrs [25]; their specific surface (courtesy of Hiroaki Sai, Cornell University, Ithaca, NY) was 137.41 ±0.17 m^2/g. The effects of each mOPN fragment on HA formation and growth was studied in gelatin gel [17,18] and pH stat [26] systems. Fl-mOPN at one concentration was included for comparison. Four different types of studies were performed in the gelatin system: comparison of the fragment to protein-free controls; comparison of HA seeds coated with the protein fragment to uncoated seeds; comparison of dephosphorylated and phosphorylated fragments; and comparison of collagen fibrils coated with fragments to uncoated-fibrils. For collagen studies, 81.25μg/ml type I rat tail collagen fibrils (BD Biosciences, Bedford MA) were pre-incubated with a concentration of each mOPN fragment corresponding to its plateau value in the *de novo* formation studies ("optimal concentration"). For seeded growth studies 0.5 mg/ml HA seeds were pre-coated with the "optimal concentration" of fragment, and following a brief wash in Tris-buffer (pH 7.4, 0.15M), the seeds included at the site of the precipitant band in the gel. For each individual set of experiments data was expressed as experimental/control.

For the pH stat studies, 3.0 mg of HA was incubated overnight in the cold with "optimal concentrations" of fragments in 250μl saline. HA with adsorbed protein was quickly washed with water, the supernatant protein concentration checked, and the pellet resuspended in 250μl water and transferred to a 10.0 ml pH stat reaction vessel containing 3mL of 2mM calcium chloride and 3mL of 2mM ammonium phosphate (pH 7.40, 25°C). The pH was maintained at 7.40 by addition of 0.1N NaOH. Rates of HA seeded growth were calculated by drawing a tangent to the steepest slope of the titration curve.

Binding of mOPN Fragments to Collagen

The mOPN fragments association with collagen fibrils was determined using binding studies with 50 ug/ml dried fibrillar collagen per micro-titer well, incubated in the presence of 1mM calcium chloride with increasing concentrations (0.05–50 ug/ml) mOPN or the N-terminal fragments, followed by washing, and detection of binding by anti-mOPN [27] followed by detection with an ALP-coupled second antibody [28]. Because the antibody did not react with the other fragments, a second set of experiments measured the binding of the Alexa-Fluor labeled (Invitrogen, Carlsbad, CA) mOPN and the N-terminal and SKK-fragments, with detection of binding by fluorescence (Perkin-Elmer 5500 fluorimeter). The amount of bound mOPN or fragment in the fluorescent studies was determined from an Alexa-Fluor standard curve and calculation of the amount bound as the difference between the equilibrated (free) and initial concentration as a function of protein added. Binding curves were calculated using Slide Write Plus Software (Advanced Graphics Software, Rancho Santa Fe, CA). Linear regressions calculated from the same software were used to calculate the affinity constant K_d, and the maximum binding, B_{max}.

Statistics

Each experiment was repeated 3–5 independent times, and average parameters from these sets of experiments determined and compared by a Student's t-test (GraphPad, San Diego, CA). Where comparing multiple experiments (varying concentrations and post-translational modification) analysis of variance (ANOVA) was followed by a Bonferroni t-test correcting for the number of variables.

RESULTS

The molecular sizes of the fl-mOPN and each of the mOPN fragments studied in these experiments are summarized in Table 1. There was no evidence that fl-mOPN was forming aggregates or higher molecular weight species. Compared to fl-mOPN which we had previously demonstrated promoted HA formation and growth [17], similar molarities of the fragments (based on comparison of curve-fit data) had distinct effects on de novo HA formation in the gelatin gel (Figure 2a). The curve-fit data in this figure also shows that at all concentrations tested the N- and C-terminal fragments promoted mineralization (relative to protein free controls); the SKK-fragment in contrast, was an inhibitor. Each fragment reached a dose-dependent plateau, with the N-terminal fragment reaching the plateau more rapidly than the C-terminal fragment. When each fragment was de-phosphorylated, experimental/control values were not significant, ranging from 0.95–1.02 (not shown).

All three fragments inhibited HA-seeded growth in the pH stat and the gelatin-gel system relative to uncoated HA (Figure 2b, Table 2). The central SKK-fragment was the most effective inhibitor in the pH stat (Figure 2b–1), but in the gelatin gel comparable molarities of the C-terminal fragment and SKK slightly inhibited seeded growth (Figure 2b–2). The N-terminal fragment only showed a significant decrease in phosphate loss relative to controls. The HA binding affinities were greatest for fl-mOPN followed by the C-terminal fragment; the number of HA-specific binding sites was greatest for SKK (Table 2).

When coated on fibrillar collagen (Figure 2c), the central SKK-fragment lost its inhibitory effect as did the C-terminal fragment, but the N-terminal fragment acted as an inhibitor. The binding affinities of mOPN and N-term mOPN based on a direct analysis using the mOPN antibody and the binding of the C-term mOPN and the SKK-fragment based on Alexa-fluor labeling yielded comparable values for the N- and C-terminal fragments; SKK and fl-mOPN had lower affinities for collagen than these fragments. (Table 2, Figure 3).

DISCUSSION

This study confirms our hypothesis that proteolytic fragments of mOPN generated by thrombin-cleavage have distinct effects on HA formation and growth. More interestingly, one fragment, the central SKK-fragment, was an inhibitor of *de novo* formation, similar to bone OPN [3], while the C- and N-terminal fragments, at all concentrations tested were *de novo* HA promoters. Interestingly, when bound to HA crystals in the concentrations studied here, the fragments, like the OPN-ASARM peptide [12] either were inhibitors or had no significant effect, suggesting the importance of the interaction between the fragments and HA.

In this study we have used proteolytic fragments of mOPN as models for providing information about the role of specific domains. In the circulation there are a variety of forms of OPN which result from enzymatic cleavage [21,29,30]. It is not known whether similar OPN fragments exist in the mineralized tissues, but fragments are the most abundant forms of OPN in bone marrow [31]. There is a collagen binding domain in OPN from aa 150–177, which is contained in the SKK-fragment [32]. Composites of this collagen binding domain and collagen induced HA formation in an agarose gel [32]. In our study, the SKK-fragment, which was the most effective inhibitor of all the fragments tested in the absence of fibrillar collagen, lost its inhibitory activity when associated with the collagen, suggesting that a change in the conformation of this domain on collagen binding might block its interaction with mineral crystals.

The conformation of OPN and the other SIBLING proteins studied to date are typical of “intrinsically disordered proteins” (IDPs) [17,33,34]. While IDPs can have domains with

more structure, their flexible nature [35] makes them suitable for interacting with many other proteins, cells, and surfaces, and enables them to be multifunctional, as is the case with mOPN. Of interest, transglutaminase treatment of mOPN decreases the disorder, while facilitating the interaction with collagen [36]. It is likely that some OPN fragments will also be IDPs, but the central region, represented by the SKK-fragment may be less random in structure. The actual structures when they interact with HA or with collagen remains to be determined.

The thrombin-cleavage region in murine, bovine, and human are highly conserved. It is thus of interest to note that the antibody to a mouse OPN thrombin cleavage fragment that blocked oxalate formation in a murine kidney stone model lies near the SKK fragment [16]. This implies that OPN folding in that domain will be important for mineral regulation. It is also of interest to note that both the N- and C-terminal fragments, although having different numbers of anionic residues, with the N- terminus being more phosphorylated, were relatively comparable in effect during *de novo* HA formation, suggesting these highly phosphorylated regions of OPN, by binding Ca, may be the most effective promoters of mineralization. In contrast, the analyzed fragments either inhibited HA-seeded growth or had no effect, probably due to their abilities to bind to HA. As expected, when dephosphorylated all fragments and the full length protein lost the abilities to act as promoters or inhibitors of mineralization demonstrating the importance of the phosphate groups for the interaction with the mineral. These results are important both for understanding the role of OPN in physiologic mineralization as well as its role in pathologic calcification.

There are limitations to the study reported here. The fragments studied were derived from mOPN, which may be distinct from the less phosphorylated forms of OPN isolated from the mineralized tissues. Recently, however, OPN purified from murine osteoblasts were shown to contain 21 phosphate groups distributed over 27 sites [37] implying that the OPN first made in bone may be more highly phosphorylated than that isolated from the mineralized tissues. Second, we used thrombin-cleavage products as models of OPN fragments; these may not be the forms that exist in the mineralized tissues. Furthermore, the protein in bone may exist in a polymeric form, and this might affect the generalizability of the findings in this paper; since we do not know how or if the polymer is fragmented. Lastly, the binding curves calculated for fragment-collagen interactions yielded similar saturation values but different shaped curves because two distinct methods of measurements were used. Those only trends can be considered. Despite all of this, the studies here serve to demonstrate that individual domains of proteins associated with mineralization may function in different ways; further studies will be required using bone isolated polymeric OPN with and without fragmentation to reach a more general conclusion.

Acknowledgments

This investigation was supported in part by USPHS Research Grant DE04141 from the National Institute of Dental and Craniofacial Research, National Institutes of Health, Bethesda, MD, 20892 (A.L.B) and by a Novo Nordisk Foundation grant, Tuborg Havnevej, 2900 Hellerup, Denmark (E.S.S.) The authors appreciate the technical contributions of students John M. DiBianco and Sylvia Ebalu and Yukiji Fujimoto to these studies.

References

1. Chen S, Chen L, Jahangiri A, Chen B, Wu Y, Chuang HH, Qin C, MacDougall M. Expression and processing of small integrin-binding ligand N-linked glycoproteins in mouse odontoblastic cells. Arch Oral Biol. 2008; 53:879–889. [PubMed: 18582847]
2. Qin C, Baba O, Butler WT. Post-translational modifications of sibling proteins and their roles in osteogenesis and dentinogenesis. Crit Rev Oral Biol Med. 2004; 15:126–136. [PubMed: 15187031]

3. Boskey AL, Maresca M, Ullrich W, Doty SB, Butler WT, Prince CW. Osteopontin-hydroxyapatite interactions in vitro: inhibition of hydroxyapatite formation and growth in a gelatin-gel. Bone Miner. 1993; 22:147–158. [PubMed: 8251766]
4. Boskey AL. Osteopontin and related phosphorylated sialoproteins: effects on mineralization. Ann N Y Acad Sci. 1995; 760:249–256. [PubMed: 7785899]
5. Hunter GK, Hauschka PV, Poole AR, Rosenberg LC, Goldberg HA. Nucleation and inhibition of hydroxyapatite formation by mineralized tissue proteins. Biochem J. 1996; 317:59–64. [PubMed: 8694787]
6. Goldberg HA, Warner KJ, Li MC, Hunter GK. Binding of bone sialoprotein, osteopontin and synthetic polypeptides to hydroxyapatite. Connect Tissue Res. 2001; 42:25–37. [PubMed: 11696986]
7. Jono S, Peinado C, Giachelli CM. Phosphorylation of osteopontin is required for inhibition of vascular smooth muscle cell calcification. J Biol Chem. 2000; 275:20197–20203. [PubMed: 10766759]
8. Boskey AL, Doty SB, Kudryashov V, Mayer-Kuckuk P, Roy R, Binderman I. Modulation of extracellular matrix protein phosphorylation alters mineralization in differentiating chick limb-bud mesenchymal cell micromass cultures. Bone. 2008; 42:1061–1071. [PubMed: 18396125]
9. Addison WN, Azari F, Sørensen ES, Kaartinen MT, McKee MD. Pyrophosphate inhibits mineralization of osteoblast cultures by binding to mineral, up-regulating osteopontin, and inhibiting alkaline phosphatase activity. J Biol Chem. 2007; 282:15872–15883. [PubMed: 17383965]
10. Jahnen-Dechent W, Schäfer C, Ketteler M, McKee MD. Mineral chaperones: a role for fetuin-A and osteopontin in the inhibition and regression of pathologic calcification. J Mol Med. 2008; 86:379–389. [PubMed: 18080808]
11. Gericke A, Qin C, Spevak L, Fujimoto Y, Butler WT, Sørensen ES, Boskey AL. Importance of phosphorylation for osteopontin regulation of biomineralization. Calcif Tissue Int. 2005; 77:45–54. [PubMed: 16007483]
12. Addison W, Masica D, Gray J, McKee MD. Phosphorylation-Dependent Inhibition of Mineralization by Osteopontin ASARM Peptides is regulated by PHEX Cleavage. J Bone Miner Res. 2010; 25:695–705. [PubMed: 19775205]
13. Boskey AL, Spevak L, Paschalis E, Doty SB, McKee MD. Osteopontin deficiency increases mineral content and mineral crystallinity in mouse bone. Calcif Tissue Int. 2002; 71:145–154. [PubMed: 12073157]
14. Matsui Y, Rittling SR, Okamoto H, Inobe M, Jia N, Shimizu T, Akino M, Sugawara T, Morimoto J, Kimura C, Kon S, Denhardt D, Kitabatake A, Uede T. Osteopontin deficiency attenuates atherosclerosis in female apolipoprotein E-deficient mice. Arterioscler Thromb Vasc Biol. 2003; 23:1029–1034. [PubMed: 12730087]
15. Wesson JA, Johnson RJ, Mazzali M, Beshensky AM, Stietz S, Giachelli C, Liaw L, Alpers CE, Couser WG, Kleinman JG, Hughes J. Osteopontin is a critical inhibitor of calcium oxalate crystal formation and retention in renal tubules. J Am Soc Nephrol. 2003; 14:139–147. [PubMed: 12506146]
16. Hamamoto S, Yasui T, Okada A, Hirose M, Matsui Y, Kon S, Sakai F, Kojima Y, Hayashi Y, Tozawa K, Uede T, Kohri K. Crucial role of the cryptic epitope SLAYGLR within osteopontin in renal crystal formation of mice. J Bone Miner Res. 2011; 26:2967–2977. [PubMed: 21898593]
17. Gericke A, Qin C, Sun Y, Redfern R, Redfern D, Fujimoto Y, Taleb H, Butler WT, Boskey AL. Different forms of DMP1 play distinct roles in mineralization. J Dent Res. 2010; 89:355–359. [PubMed: 20200415]
18. Boskey AL, Chiang P, Fermanis A, Brown J, Taleb H, David V, Rowe PS. MEPE's diverse effects on mineralization. Calcif Tissue Int. 2010; 86:42–46. [PubMed: 19998030]
19. Boskey AL, Maresca M, Doty S, Sabsay B, Veis A. Concentration-dependent effects of dentin phosphophoryn in the regulation of in vitro hydroxyapatite formation and growth. Bone Miner. 1990; 11:55–65. [PubMed: 2176557]

20. Boskey A, Spevak L, Tan M, Doty SB, Butler WT. Dentin sialoprotein (DSP) has limited effects on in vitro apatite formation and growth. Calcif Tissue Int. 2000; 67:472–478. [PubMed: 11289697]
21. Christensen B, Schack L, Klaning E, Sørensen ES. Osteopontin is cleaved at multiple sites close to its integrin-binding motifs in milk and is a novel substrate for plasmin and cathepsin D. J Biol Chem. 2010; 285:7929–7937. [PubMed: 20071328]
22. Sørensen ES, Højrup P, Petersen TE. Posttranslational modifications of bovine osteopontin: identification of twenty-eight phosphorylation and three O-glycosylation sites. Protein Sci. 1995; 4:2040–2049. [PubMed: 8535240]
23. Christensen B, Nielsen MS, Haselmann KF, Petersen TE, Sørensen ES. Post-translationally modified residues of native human osteopontin are located in clusters: identification of 36 phosphorylation and five O-glycosylation sites and their biological implications. Biochem J. 2005; 390:285–292. [PubMed: 15869464]
24. Sørensen ES, Petersen TE. Purification and characterization of three proteins isolated from the proteose peptone fraction of bovine milk. J Dairy Res. 1993; 60:189–197. [PubMed: 8320368]
25. Blumenthal NC, Betts F, Posner AS. Formation and structure of Ca-deficient hydroxyapatite. Calcif Tissue Int. 1981; 33:111–117. [PubMed: 6260311]
26. Millan AM, Sugars RV, Embery G, Waddington RJ. Adsorption and interactions of dentine phosphoprotein with hydroxyapatite and collagen. Eur J Oral Sci. 2006; 114:223–231. [PubMed: 16776772]
27. Schack L, Lange A, Kelsen J, Agnholt J, Christensen B, Petersen TE, Sørensen ES. Considerable variation in the concentration of osteopontin in human milk, bovine milk and infant formulas. J Dairy Science. 2009; 92:5378–5385.
28. Rosenberg K, Olsson H, Mörgelin M, Heinegård D. Cartilage oligomeric matrix protein shows high affinity zinc-dependent interaction with triple helical collagen. J Biol Chem. 1998; 273:20397–20403. [PubMed: 9685393]
29. Agnihotri R, Crawford HC, Haro H, Matrisian LM, Havrda MC, Liaw L. Osteopontin, a novel substrate for matrix metalloproteinase-3 (stromelysin-1) and matrix metalloproteinase-7 (matrilysin). J Biol Chem. 2001; 276:28261–28267. [PubMed: 11375993]
30. Plumer A, Duan H, Subramaniam S, Lucas FL, Miesfeldt S, Ng AK, Liaw L. Development of fragment-specific osteopontin antibodies and ELISA for quantification in human metastatic breast cancer. BMC Cancer. 2008; 8:38. [PubMed: 18237408]
31. Grassinger J, Haylock DN, Storan MJ, Haines GO, Williams B, Whitty GA, Vinson AR, Be CL, Li S, Sørensen ES, Tam PP, Denhardt DT, Sheppard D, Choong PF, Nilsson SK. Thrombin-cleaved osteopontin regulates hemopoietic stem and progenitor cell functions through interactions with alpha9beta1 and alpha4beta1 integrins. Blood. 2009; 114:49–59. [PubMed: 19417209]
32. Lee JY, Choo JE, Choi YS, Park JB, Min DS, Lee SJ, Rhyu HK, Jo IH, Chung CP, Park YJ. Assembly of collagen-binding peptide with collagen as a bioactive scaffold for osteogenesis in vitro and in vivo. Biomaterials. 2007; 28:4257–4267. [PubMed: 17604098]
33. Fisher LW, Torchia DA, Fohr B, Young MF, Fedarko NS. Flexible structures of SIBLING proteins, bone sialoprotein, and osteopontin. Biochem Biophys Res Commun. 2001; 280:460–465. [PubMed: 11162539]
34. Yamaguchi Y, Hanashima S, Yagi H, Takahashi Y, Sasakawa H, Kurimoto E, Iguchi T, Kon S, Uede T, Kato K. NMR characterization of intramolecular interaction of osteopontin, an intrinsically disordered protein with cryptic integrin-binding motifs. Biochem Biophys Res Commun. 2010; 393:487–491. [PubMed: 20152802]
35. Tompa, P. Structure and Function of Intrinsically Disordered Proteins. CRC Press, Taylor & Frances; NY: 2010.
36. Kaartinen MT, Pirhonen A, Linnala-Kankkunen A, Mäenpää PH. Cross-linking of osteopontin by tissue transglutaminase increases its collagen binding properties. J Biol Chem. 1999; 274:1729–1735. [PubMed: 9880554]
37. Christensen B, Kazanecki C, Petersen TE, Rittling SR, Denhardt DT, Sørensen ES. Cell-type specific post-translational modifications of mouse osteopontin are associated with different adhesive properties. J Biol Chem. 2007; 282:19463–19472. [PubMed: 17500062]

HIGHLIGHTS

- Thrombin-cleaved fragments of milk-Osteopontin effect hydroxyapatite formation differently
- N- and C- terminal fragments promoted hydroxyapatite formation and growth
- A central fragment inhibited hydroxyapatite formation and growth
- Binding to collagen or hydroxyapatite seed crystals modified these effects

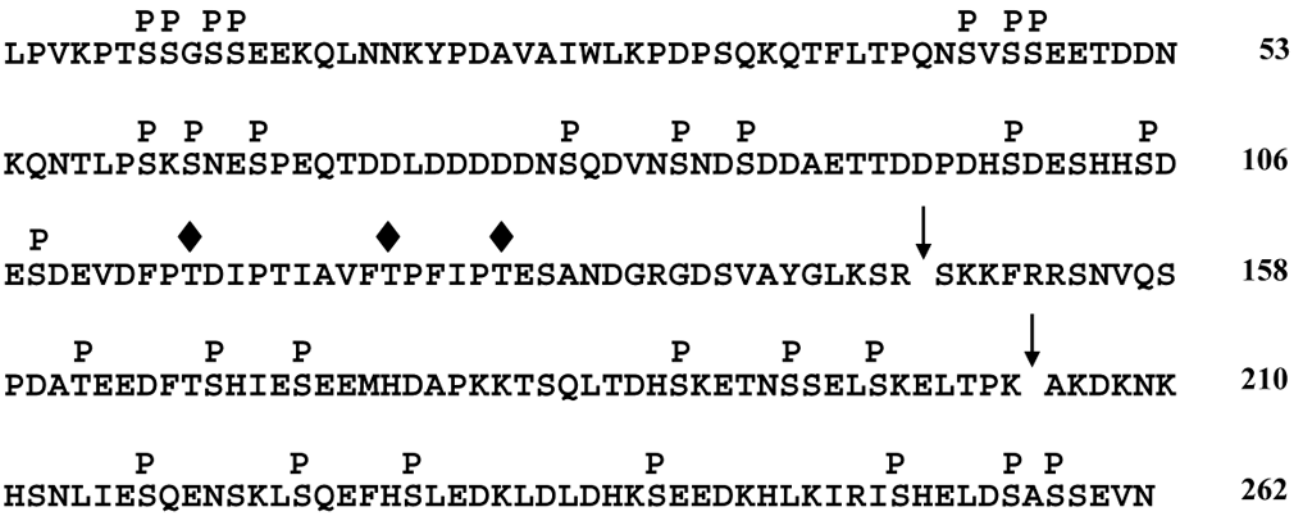

Figure 1. Primary sequence of bovine milk osteopontin

Thrombin cleavage sites generating the N-terminal (aa 1–147), central SKK-, (aa 148–204), and C-terminal (205–262) fragments are indicated with arrows. Phosphorylation and glycosylation sites identified in bovine milk OPN are indicated with P's and diamonds, respectively.

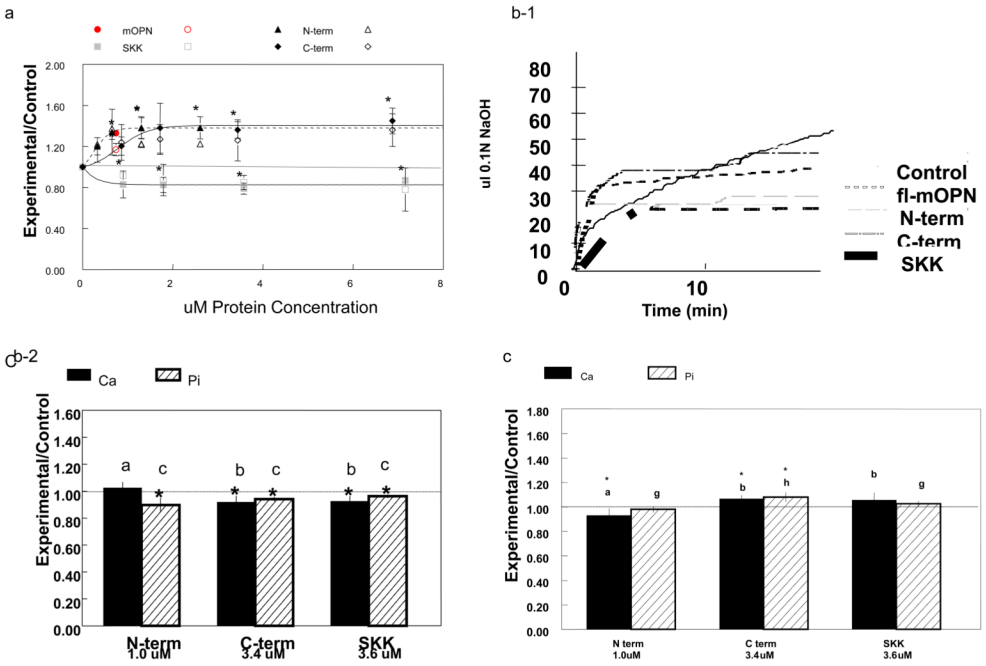

Figure 2.

(a) Concentration dependent effects of OPN fragments on HA formationin the gelatin gel system normalized to protein free control (Experimental/Control). All data were obtained at 5.0 days in the presence of variable concentrations of the C- and N- terminal fragments (C-term, N-term) or the central SKK-fragment (SKK). A single concentration is shown for full length (fl-)mOPN. Closed shapes represent Ca concentrations, open shapes represent Pi concentrations, all values are ±SD, n=5. Circle – fl-mOPN, upward triangle – N terminal fragment, diamond – C-terminal fragment, square- SKK- fragment. * $p<0.05$ relative to protein-free controls is shown only for Ca concentrations. All lines were determined by curve-fitting and had R^2 >0.89.

(b) Effects of OPN fragments on HA seeded growth. (1) With the exception of the N-terminal fragment, 0.5mg/ml HA seeds coated with the indicated concentrations of fragments showed small but significant decreases compared to uncoated HA in the gelatin-gel. All values are mean ±SD, n=3. * $p<0.05$ relative to protein-free HA-seeded control; equivalent letters are not significantly different from each other. The dotted line shows control value. **(2)** Effects in the pH Stat at room temperature. The lines are averages of 3–5 replicates, and represent experiments using the same concentrations as indicated in figure (2b(1)) for fl-mOPN, C-terminal, N-terminal, and SKK fragments.

(**c) Interaction with fibrillar collagen alters OPN fragments effects on HA formation**. Using the concentration at which each curve in figure a reached a plateau to coat fibrillar collagen fragments, the effects of the fragments on collagen mediated mineralization were compared to fibrillar collagen alone (*$p<0.05$). Bars marked with similar letters were not significantly different from one another (Bonferroni multiple comparisons test) Dotted line is control value.

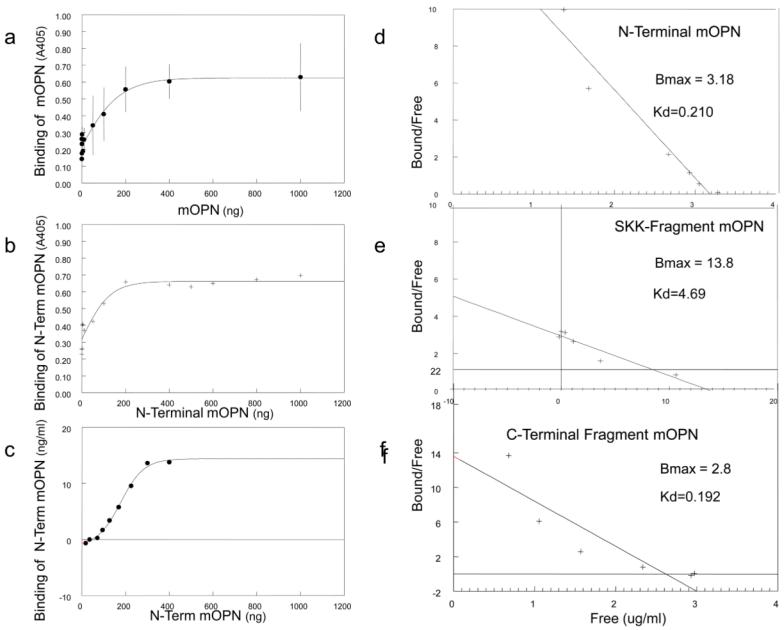

Figure 3. Affinity of OPN fragments for collagen

(A) Binding curves of mOPN to type I collagen monitored using a primary mOPN antibody visualized using an anti-rabbit IgG-alkaline phosphatase conjugate with p-nitrophenyl phosphate as substrate. The enzyme activity is indicated by the A405 absorbance. (B) Similar binding curves for the N-terminal fragment binding to type I collagen. C) Binding curves calculated based on the presence of the fluorescent N-terminal fragment. D) Binding curves calculated based on the presence of the fluorescence SKK fragment. See table 2 for calculated affinities.

Table 1

Thrombin cleavage of bovine OPN

Full length mOPN and the fragments generated by thrombin cleavage of bovine mOPN were separated by gel filtration and RP-HPLC, and subsequently characterized by N-terminal sequence and MALDI-TOF-MS analyses. The observed molecular masses were determined by MALDI-TOF-MS in linear mode. Mass difference is that between the observed calculated average masses before and after treatment with alkaline phosphatase. The number of phosphorylations corresponding to the mass difference is given in parentheses:

Fragment	ALP	Observed mass (Da)	Calculated mass (Da)	Mass difference (Da)
Leu^{1}-Asn^{262} (Full-length)	−	~33,900	29,284	1,700 (21–22)
	+	~32,200		
Leu^{1}-Arg^{147} (N-terminal)	−	~19,200	16,103	~800 (10)
	+	~18,400		
Ser^{148}-Lys^{204} (Central/SKK)	−	6986.5/6905.4/6824.6	6506.0	480.7/399.6/318.8(6/5/4)
	+	6505,8		
Ala^{205}-Asn^{262} (C-terminal)	−	7273.7/7192.9/7112.6	6713.3	560.7/479.9/399.6(7/6/5)
	+	6713.0		

Table 2

Effect of mOPN Fragments on Collagen Binding and HA Seeded Growth

	mOPN-Collagen Interactions Binding Constants[a]			pH Stat Studies[b]
	Bmax (nM)	**K_d (nM)**	**R^2**	**Rate of HA Formation (ul/min)**
(fl) mOPN	1.21	0.42	0.80	0.39±0.003[c]
N-term	3.18	0.210	0.94	0.23±0.007[c]
C-term	2.81	0.192	0.79	0.48±0.005[c]
SKK	13.8	4.69	0.93	0.0038±0.001[c]

[a] Binding constants calculated from plots of bound/free vs. bound. K_d is the equilibrium constant at which ½ the binding sites are filled, B_{max} is the specific binding, and R^2 indicates the goodness of fit.

[b] Kinetics of seeded growth measured from the initial slope of base addition, mean ± SD

[c] $p<0.05$ significantly different than uncoated HA seeds (rate 1.98 ul/min);